31st Annual International Conference of the IEEE EMBS
Minneapolis, Minnesota, USA, September 2-6, 2009

Time-Varying Spectrum Estimation of Heart Rate Variability Signals with Kalman Smoother Algorithm

M.P. Tarvainen*[1], S. Georgiadis[1], J.A. Lipponen[1], M. Hakkarainen[1] and P.A. Karjalainen[1]

[1]Department of Physics, University of Kuopio, Kuopio, Finland

Abstract— **A time-varying parametric spectrum estimation method for analyzing dynamics of heart rate variability (HRV) signals is presented. In the method, HRV signal is first modeled with a time-varying autoregressive model and the model parameters are solved recursively with a Kalman smoother algorithm. Time-varying spectrum estimates are then obtained from the estimated model parameters. The obtained spectrum can be further decomposed into separate components, which is especially advantageous in HRV applications where low frequency (LF) and high frequency (HF) components are generally aimed to be distinguished. As case studies, the dynamics of HRV signals recorded during 1) orthostatic test, 2) exercise test and 3) simulated driving task are analyzed.**

I. INTRODUCTION

Heart rate variability (HRV) is a result of autonomic nervous system and humoral effects on the sinus node. The autonomic nervous system can be divided into parasympathetic (also called vagal) and sympathetic branches. Roughly speaking, sympathetic activity tends to increase heart rate (HR↑) and parasympathetic tends to decrease it (HR↓) [1]. The most conspicuous periodic component of HRV is the respiratory sinus arrhythmia (RSA) which is considered to range from 0.15 to 0.4 Hz. This high frequency (HF) component is generally believed to be mediated predominantly by parasympathetic activity [1]. Another apparent component of HRV is the low frequency (LF) component ranging from 0.04 to 0.15 Hz. The rhythms within the LF band are nowadays generally thought of being both of sympathetic and parasympathetic origin [1]. Thus, HRV is commonly examined through spectral analysis and, e.g., the LF/HF ratio is sometimes considered as an index of sympatho-vagal balance.

Due to the complex control systems of HRV, it is presumable that the characteristics of HRV (e.g. the powers and frequencies of LF and HF components) vary in time. Especially, changes in physiological conditions may produce significant variations. For example, in the orthostatic test, where subject stands up after lying supine for few minutes, an increase in HR compensates the decrease in blood pressure taking place after standing up. On supine, the HF component of HRV is typically strong, often stronger than the LF component. At the instant of standing up, an immediate strong decrease in HF component and a more gradual increase in LF component has been observed [2]. In addition, HRV is known to be affected by both physical [3] and mental stress [4]. In order to analyze such changes time-frequency methods are required.

In this paper, we present a Kalman smoother method for estimating time-varying characteristics of HRV. In the method, HRV signal is first modeled with a time-varying autoregressive (AR) model. The parameters of the model are estimated with a Kalman smoother algorithm. The time-varying spectrum is then obtained from the estimated model parameters. Furthermore, the obtained spectrum can be decomposed into separate frequency components, and thus, dynamics of LF and HF components can be analyzed without applying any fixed frequency bands.

II. METHODS

The formulation of Kalman smoother algorithm is based on a state-space formalism. Basically this means that we have an observation model for the data (i.e. space equation) and also a model for the evolution of the observation model parameters (i.e. state equation). In the following, a short description of the Kalman smoother spectrum estimation approach is given (for details see [5]).

The HRV signal is first modeled with a time-varying AR model of order p defined as

$$x_t = -\sum_{j=1}^{p} a_t^{(j)} x_{t-j} + e_t \tag{1}$$

where x_t is the modeled signal (i.e. RR interval series in this case), $a_t^{(j)}$ is the value of j'th AR parameter at time t and e_t is observation error. By denoting

$$H_t = (x_{t-1}, \ldots, x_{t-p}) \tag{2}$$

$$\theta_t = (-a_t^{(1)}, \ldots, -a_t^{(p)})^T \tag{3}$$

the time-varying AR model can be written in the form

$$x_t = H_t \theta_t + e_t \tag{4}$$

which is a linear observation model. The evolution of the state (i.e. AR parameters) is here modeled with a random walk model

$$\theta_{t+1} = \theta_t + w_t \tag{5}$$

where w_t is a state noise term. Equations (4) and (5) form the state-space signal model for the time-varying AR process x_t and the evolution of the AR parameters can now be estimated by using the Kalman smoother algorithm.

*M.P. Tarvainen is with the Department of Physics, University of Kuopio, P.O.Box 1627, FI-70211 Kuopio, Finland (mika.tarvainen@uku.fi).

978-1-4244-3296-7/09/$25.00 ©2009 IEEE

A. Kalman smoother algorithm

The Kalman smoother algorithm consists of a Kalman filter algorithm and a fixed-interval smoother. The Kalman filtering problem is to find the linear mean square estimator $\hat{\theta}_t$ for state θ_t given observations $x_1, x_2, \ldots, x_t$. Kalman filter equations can be summarized as

$$C_{\tilde{\theta}_{t|t-1}} = C_{\tilde{\theta}_{t-1}} + C_{w_{t-1}} \quad (6)$$

$$K_t = C_{\tilde{\theta}_{t|t-1}} H_t^T (H_t C_{\tilde{\theta}_{t|t-1}} H_t^T + C_{e_t})^{-1} \quad (7)$$

$$\hat{\theta}_t = \hat{\theta}_{t-1} + K_t(x_t - H_t \hat{\theta}_{t-1}) \quad (8)$$

$$C_{\tilde{\theta}_t} = (I - K_t H_t) C_{\tilde{\theta}_{t|t-1}} \quad (9)$$

where $\tilde{\theta}_t$ is the state estimation error $\tilde{\theta}_t = \theta_t - \hat{\theta}_t$, $\tilde{\theta}_{t|t-1}$ is the state prediction error $\tilde{\theta}_{t|t-1} = \theta_t - \hat{\theta}_{t-1}$, K_t is the Kalman gain vector, and C_{e_t} and C_{w_t} are the observation and state noise covariances, respectively.

The fixed-interval smoothing problem is to find estimates $\hat{\theta}_t^{\mathrm{S}}$ (S denotes smoothed estimates) for each state θ_t given all the observations $x_1, x_2, \ldots, x_N$. Fixed-interval smoothing equations can be summarized as

$$\hat{\theta}_t^{\mathrm{S}} = \hat{\theta}_t + A_t(\hat{\theta}_{t+1}^{\mathrm{S}} - \hat{\theta}_t) \quad (10)$$

$$C_{\tilde{\theta}_t^{\mathrm{S}}} = C_{\tilde{\theta}_t} + A_t(C_{\tilde{\theta}_{t+1}^{\mathrm{S}}} - C_{\tilde{\theta}_{t+1|t}}) A_t^T \quad (11)$$

where $A_t = C_{\tilde{\theta}_t} C^{-1}_{\tilde{\theta}_{t+1|t}}$ and filtered estimates are used for initialization, i.e. $\hat{\theta}_N^{\mathrm{S}} = \hat{\theta}_N$ and $C_{\tilde{\theta}_N^{\mathrm{S}}} = C_{\tilde{\theta}_N}$.

B. Adaptation of the algorithm

The terms effecting the adaptation of Kalman smoother algorithm are the state and observation noise covariances C_{w_t} and $C_{e_t} = \sigma_{e_t}^2$, respectively. The observation noise variance can be estimated iteratively at every step of the Kalman filter equations as

$$\hat{\sigma}_{e_t}^2 = 0.95\, \hat{\sigma}_{e_{t-1}}^2 + 0.05\, \epsilon_t^2 \quad (12)$$

where ϵ_t is the one step prediction error $\epsilon_t = x_t - H_t \hat{\theta}_{t-1}$. Furthermore, the state noise covariance is selected to be diagonal $C_{w_t} = \sigma_{w_t}^2 I$ and $\sigma_{w_t}^2$ is adjusted at every step of the Kalman filter equations as

$$\hat{\sigma}_{w_t}^2 = \mathrm{UC}\, \hat{\sigma}_{e_t}^2 / \hat{\sigma}_{x_t}^2 \quad (13)$$

where $\hat{\sigma}_{x_t}^2$ is the estimated variance of the observed RR series at time t and UC is an update coefficient through which the adaptation of the algorithm can be adjusted.

C. Time-varying spectrum estimation

The time-varying spectrum estimate is obtained from the time-varying AR parameter estimates $\hat{a}_t^{(j)}$ as

$$P_t(f) = \frac{\hat{\sigma}_{e_t}^2 / f_s}{|1 + \sum_{j=1}^{p} \hat{a}_t^{(j)} e^{-i2\pi j f / f_s}|^2} \quad (14)$$

where f_s is the sampling frequency, $\hat{a}_t^{(j)}$ is the j'th AR parameter estimate at time t, and $\hat{\sigma}_{e_t}^2$ is the posterior variance of the observation error process (i.e. computed by using the smoothed estimates).

D. Spectral decomposition

One property of AR spectrum estimation methods, that is especially advantageous in HRV applications, is that the spectrum can be divided into separate components as follows. Equation (14) can also be written in the factored form

$$P_t(f) = \frac{\hat{\sigma}_{e_t}^2 / f_s}{\prod_{j=1}^{p} (z - \alpha_t^{(j)})(1/z - \alpha_t^{(j)*})} \quad (15)$$

where $z = e^{i2\pi f / f_s}$, $\alpha_t^{(j)}$ are the time-varying roots of the AR polynomial (also called poles), and * denotes complex conjugate. Now, consider a pole $\alpha_t^{(j)}$ positioned at frequency f_j. The spectrum of this single component in the vicinity of f_j can be estimated by assuming the effect of other poles on the spectrum to be constant (for details see [5]). The powers of the spectral components are finally estimated by simply evaluating the areas of the components.

III. Results

The Kalman smoother spectrum estimation method was applied to three different case studies. Each case study and the results obtained are presented shortly in the following.

A. Case study 1: orthostatic test

In the test, subject (a healthy young male) first lay supine for over five minutes and then stood up. After standing of about five minutes the subject held his breath for 30 seconds. The ECG signal was measured using a SynAmps^2 Neuroscan system (Compumedics Limited). ECG electrodes were placed according to the conventional 12 lead system with the Mason-Likar modification. For analysis, the chest lead V4 was chosen. The sampling rate of the ECG signal was 1000 Hz. The R-waves were then extracted from the ECG signal by using a QRS detection algorithm and the obtained RR interval series was interpolated with a 4 Hz cubic spline (in order to have evenly sampled signal). Furthermore, the trend within the RR series was removed by using a smoothness priors method [6]. The RR interval series and the estimated trend are shown in Fig. 1 (a).

The Kalman smoother spectrum estimate was then calculated (AR model order $p = 16$ and update coefficient UC=$1 \cdot 10^{-5}$ were used in all case studies). Respiration rate was estimated from the ECG (ECG derived respiration, EDR) in order to guide the selection of the HF component within spectral decomposition. The Kalman smoother spectrum with the EDR curve and the HF and LF component spectra are shown in Fig. 1 (b). Finally, HF and LF component powers were evaluated through numerical integration. These component powers and the LF/HF ratio are shown in Fig. 1 (c). The results show a decrease in HF power and an increase in LF power after standing up, as was expected.

B. Case study 2: exercise test

The exercise ECG recording was performed by using a Cardiovit CS-200 ergo-spirometer system (Schiller AG) with Ergoline Ergoselect 200 K bicycle ergometer. ECG electrodes were placed according to the conventional 12 lead

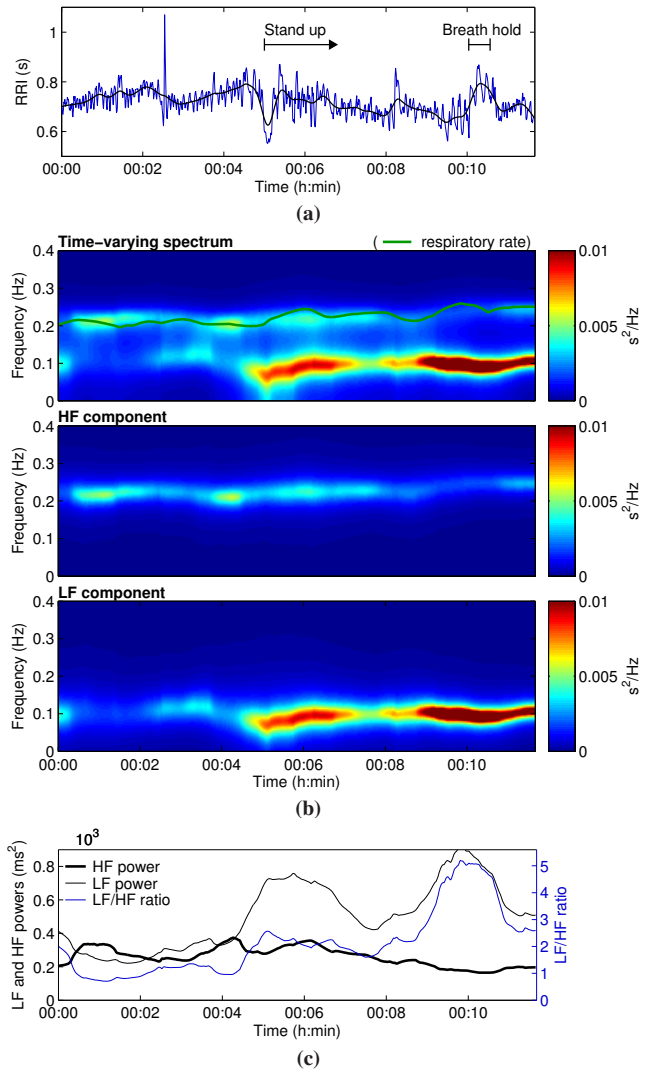

Fig. 1. Case study 1: orthostatic test with 30 second breath hold. (a) RR interval series (black line shows the removed trend), (b) Kalman smoother spectrum and respiration rate estimate (top), HF (middle) and LF (bottom) component spectra, and (c) LF and HF band powers and LF/HF ratio.

system with the Mason-Likar modification and for analysis chest lead V4 was chosen. The sampling rate of the ECG was 500 Hz. In the stepwise test procedure, subject (a healthy young male) first sat still on the bicycle for a while and then subject started the actual exercise part in which the load of the bicycle was increased with 40 W every three minutes. Subject continued exercise until exhaustion, after which the exercise test was stopped and a 10-minute recovery period was measured. Similar preprocessing steps were performed for the data as in the first case study (R-wave detection, interpolation, and detrending). Obtained RR interval series (with estimated trend) and the exercise protocol are shown in Fig. 2 (a).

The Kalman smoother spectrum estimate was then calculated similarly as for the first case study. The Kalman smoother spectrum with the EDR curve and the HF and LF component spectra for the exercise data are shown in Fig. 2 (b). Furthermore, HF and LF component powers and LF/HF ratio are shown in Fig. 2 (c). Note that in this case, power values are presented in decibels in order to have a general view of HRV dynamics during exercise (including what happens near peak exercise). The results show a prevalence of HF component compared to LF component during heavy exercise. Similar HF prevalence was reported in [3], where mechanical effect of breathing rate to the sinus node was concluded to be the most conceivable cause.

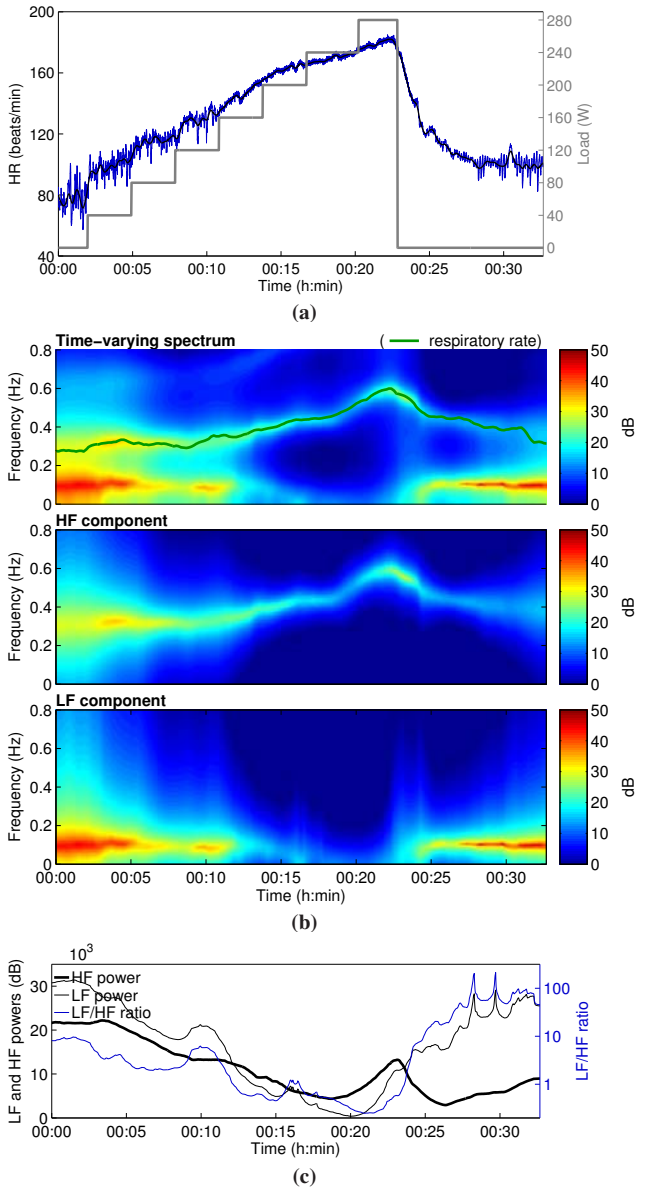

Fig. 2. Case study 2: exercise test. (a) RR interval series (black line shows the removed trend) and bicycle load during the exercise test protocol, (b) Kalman smoother spectrum and respiration rate estimate (top), HF (middle) and LF (bottom) component spectra, and (c) LF and HF band powers and LF/HF ratio.

C. Case study 3: driving simulation

In the driving simulation, subject (a healthy young male) performed a driving task consisting of three driving modes: slow→normal→fast→fast→normal→slow. Each mode lasted 10 minutes, plus the time taken to finish the lap,

and between the modes there was a 3-minute break. The driving simulator is based on standard consumer products (GTR2 PC game, Logitech MOMO steering wheel/pedals), but it is set up inside a modern laboratory consisting of a sound proof room (where the driver sits) and a separate control room (where the test can be supervised). The ECG signal, along with a set of other biosignals, was measured using a ME6000 system (Mega Electronics Ltd). The sampling rate of the ECG signal was 1000 Hz. Similar preprocessing steps were performed for the data as in the previous case studies (R-wave detection, interpolation, and detrending). Obtained RR interval series and the driving task are shown in Fig. 3 (a).

The Kalman smoother spectrum with the EDR curve and the HF and LF component spectra for the driving simulation data are shown in Fig. 3 (b). Furthermore, HF and LF component powers and LF/HF ratio are shown in Fig. 3 (c). It is observed that the LF power is increased when chancing from slow to normal, and from normal to fast driving mode. In the HF power, on the other hand, an overall slight decrease is observed. In addition, the 3-minute breaks between the driving modes, where the subject sat tight and relaxed, seem to produce slight decreases in both respiration rate and HR, and also at some points slight increases in overall HRV (both LF and HF powers increase). These results are in line with the general knowledge that HRV decreases in tasks linked with physical or mental loading.

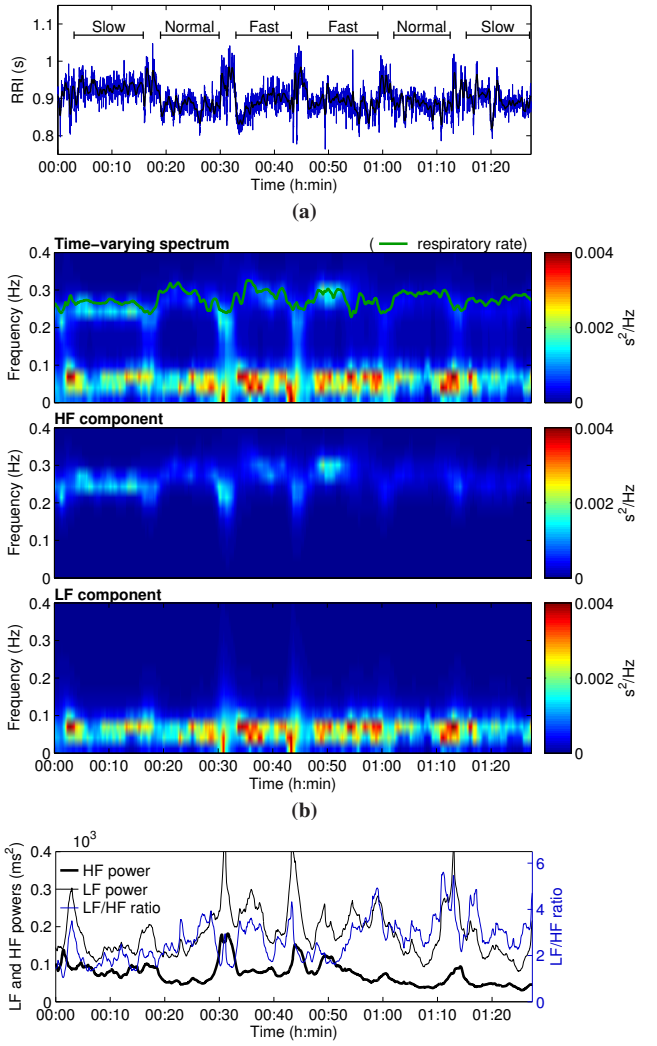

Fig. 3. Case study 3: driving simulation. (a) RR interval series (black line shows the removed trend), (b) Kalman smoother spectrum and respiration rate estimate (top), HF (middle) and LF (bottom) component spectra, and (c) LF and HF band powers and LF/HF ratio.

IV. Conclusions

A Kalman smoother algorithm based time-varying spectrum estimation method was presented. Considering parametric spectrum estimation methods based on time-varying AR model, the Kalman smoother is a statistically optimal method for estimating the model parameters. Another advantage of the Kalman smoother approach is that the spectrum can be decomposed into separate frequency components, i.e. LF and HF components of HRV can be separated. The method is computationally demanding, but when tuned correctly it can be easily applied to different data as demonstrated in this paper.

Acknowledgments

This study was supported by Academy of Finland (project number 126873, 1.1.2009-31.12.2011 and project number 123579, 1.1.2008-31.12.2011).

References

[1] G. Berntson, J. B. Jr., D. Eckberg, P. Grossman, P. Kaufmann, M. Malik, H. Nagaraja, S. Porges, J. Saul, P. Stone, and M. V. D. Molen, "Heart rate variability: Origins, methods, and interpretive caveats," *Psychophysiol*, vol. 34, pp. 623–648, 1997.

[2] L. Keselbrener and S. Akselrod, "Selective discrete Fourier transform algorithm for time-frequency analysis: method and application on simulated and cardiovascular signals," *IEEE Trans Biomed Eng*, vol. 43, no. 8, pp. 789–802, August 1996.

[3] F. Cottin, C. Médigue, P.-M. Leprêtre, Y. Papelier, J.-P. Koralsztein, and V. Billat, "Heart rate variability during exercise performed below and above ventilatory threshold," *Med Sci Sports Exerc*, vol. 36, no. 4, pp. 594–600, 2004.

[4] M. Orsila, M. Virtanen, T. Luukkala, M. Tarvainen, P. Karjalainen, J. Viik, M. Savinainen, and C. Nygård, "Perceived mental stress and reactions in heart rate variability - A pilot study among employees of an electronics company," *Int J Occup Safety Ergonomics*, vol. 14, no. 3, pp. 275–283, 2008.

[5] M. Tarvainen, S. Georgiadis, P. Ranta-aho, and P. Karjalainen, "Time-varying analysis of heart rate variability signals with Kalman smoother algorithm," *Physiol Meas*, vol. 27, no. 3, pp. 225–239, 2006.

[6] M. Tarvainen, P. Ranta-aho, and P. Karjalainen, "An advanced detrending method with application to HRV analysis," *IEEE Trans Biomed Eng*, vol. 49, no. 2, pp. 172–175, February 2002.